NJC

New Journal of Chemistry

A journal for new directions in chemistry

Accepted Manuscript

This article can be cited before page numbers have been issued, to do this please use: K. A. Chiaw, S. Basappa, M. V. Mane, K. Huang, N. J. Long and S. S. Gholap, *New J. Chem.*, 2026, DOI: 10.1039/D6NJ01950A.

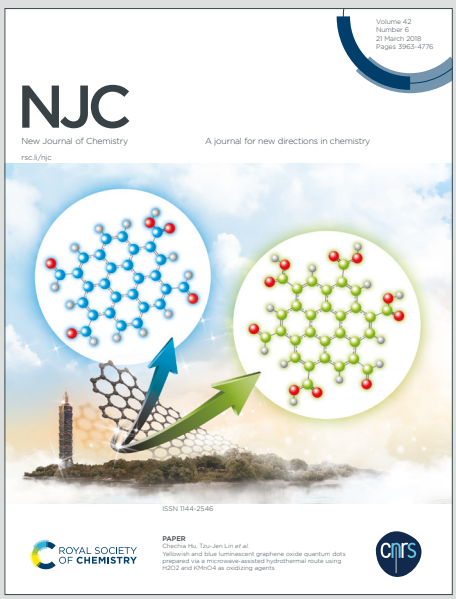

View Article Online
DOI: 10.1039/D6NJ01950A

COMMUNICATION

Alkane Dehydrogenation Catalyzed by PN^{3}P Pincer Iridium Hydride Complex

Received 00th January 20xx,
Accepted 00th January 20xx

DOI: 10.1039/x0xx00000x

Kher Ai Chiaw,[a] Suma Basappa,[b] Manoj V. Mane,[b] Kuo-Wei Huang,*[c] Nicholas Long,*[d] Sandeep Suryabhan Gholap*[a]

The use of iridium-based pincer complex, specifically the PN^{3}P pincer ligand backbone, for the efficient alkane dehydrogenation reaction is explored. Herein, we investigate the catalytic performance of PN^{3}P pincer iridium dihydride complex (Ir2) in the dehydrogenation reaction of cyclooctane to cyclooctene. With 0.1 mol% of Ir2, cyclooctane with *tert*-butylethylene (TBE) as a hydrogen acceptor and NaO^{t}Bu as a base, we achieved conversion up to 55% of *tert*-butylethylene (TBE) with TON up to 546. These results highlight the potential of PN^{3}P pincer iridium dihydride complex as a robust catalyst for selective alkane dehydrogenation under mild reaction conditions. Furthermore DFT calculations strongly support our proposed mechanism.

Alkane dehydrogenation (AD) is one of the most important reactions in the petrochemical industry as it uses abundant alkane to produce valuable olefins that are chemically versatile and can act as intermediates in higher value alkanes synthesis through olefin coupling.[1, 2] This reaction can also serve as an alternative pathway for high-temperature steam cracking of alkanes, which are energy-consuming and produce several undesirable side-products.[3] In the case of alkane dehydrogenation, molecular hydrogen (H_2) is produced as the primary by-product along with olefins. H_2 is one of the rising energy carriers owing to its high energy density and environmentally benign nature.[4] While significant efforts have been devoted to hydrogen production such as via water splitting[5a], methane pyrolysis[5b] and biomass gasification[5c], AD can eventually also serve as an attractive alternative pathway for H_2 generation. Despite the attractive advantages of the dehydrogenation of alkane to alkene and H_2, it is a highly endothermic process,[6] and this characteristic is a serious hindrance to the wide implementation of this reaction.

There are some examples of metal complexes developed over the past few decades for the dehydrogenation of alkanes, including those used with hydrogen acceptors, UV and irradiation.[7, 8] However, those complexes that contains PCP pincer type of ligand utilized with a hydrogen acceptor emerges at the top, outperforming in terms of stability, TONs and selectivity.[2, 9] Pincer ligands incorporating iridium are often used in the catalytic dehydrogenation systems given their outstanding catalytic activity and stability.[7, 10-15] Over the past decade, the high-valent oxidation state of iridium has been extensively explored for the catalytic dehydrogenation of alkanes.[16-23]

Early work by Jensen and Kaska in 1996 has demonstrated the potential of such systems.[16a] They first synthesized complex **2** from **1** in the presence of H_2 and $LiBEt_3H$, where the iridium dihydride complex **2** has shown greater stability with no observable decomposition over a week whereas the hydrochloride precursor 1 showed significant decomposition after 24h. These foundational studies have established the grounds of pincer-iridium catalysts, enabling further detailed mechanistic investigations on this catalytic system.

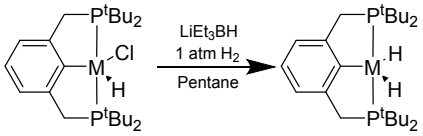

M = Ru, Ir

1 **2**

In 2021, Goldmann and co-worker reported alkane dehydrogenation catalysed by (^{t}Bu$_4$POCOP)Ir complex that proceeded through a proton-coupled electron-transfer (PCET) pathway using oxidants and bases as a proton and electron acceptor.[24] In a subsequent study, they investigated the intramolecular C(sp^3)-H activation during alkane dehydrogenation using (*p*-pyridyl-^{t}BuPCP)-IrCl$^+$ cation (*p*-

[a] Institute of Sustainability for Chemical, Energy and Environment (ISCE^2), Agency of Science, Technology and Research (A*STAR), 1 Pesek Road, Jurong Island, Singapore 627833, Singapore.
[b] Centre for Nano and Material Sciences, Jain (Deemed-to-be University), Bangalore, Karnataka 562112, India
[c] Center for Renewable Energy and Storage Technology, Division of Physical Sciences and Engineering, King Abdullah University of Science and Technology, Thuwal, 23955-6900 Saudi Arabia, Saudi Arabia.
[d] Department of Chemistry, Imperial College London, White City Campus, London, W12 0BZ, United Kingdom.
Email: sandeep_gholap@isce2.a-star.edu.sg; hkw@kaust.edu.sa; n.long@imperial.ac.uk
Footnotes relating to the title and/or authors should appear here.
Electronic Supplementary Information (ESI) available: [details of any supplementary information available should be included here]. See DOI: 10.1039/x0xx00000x

View Article Online
DOI: 10.1039/D6NJ00950A

pyridyl-^{t}BuPCP=3,5-*bis*(di-tertbutylphosphinomethyl)-2,6-dimethylpyridin-4-yl) complexes.[25] In 2022, the same group further expanded this chemistry by reporting a *bis*(2-di-tertbutyl-phosphinophenyl)phosphine (^{t}BuP^{H}PP) iridium complex for the dehydrogenation of alkane and demonstrated that the C-H activation using Ir(III) complex with the more crowded ((^{t}Bu$_4$PCP)IrCl$^+$ (^{R}PCP = 2,6-C$_6$H$_3$(CH$_2$PR$_2$) undergoes intramolecular whereas the less crowded (^{i}Pr$_4$PCP)IrCl$^+$ undergoes intermolecular C-H activation.[9, 19]

Metal-ligand cooperativity (MLC) plays an important role in C-H bond activation by enabling reversible ligand participation during catalysis.[26-33] In the case of pyridine-based pincer complex, the MLC involves in the aromatization-dearomatization pyridine ring resulting in more efficient activation of various bonds.[29, 34-51] PN^{3}P pincer complexes have previously demonstrated great performance in various chemical reactions, particularly in CO_2 hydrogenation[52] and formic acid dehydrogenation.[53] Herein, we report catalytic activity of PN^{3}P-pincer iridium complex towards dehydrogenation of alkane (Figure 1) and the evaluation of PN^{3}P-pincer iridium complexes **Ir1, Ir2** and **Ir3** for the alkane dehydrogenation. (Table 1).

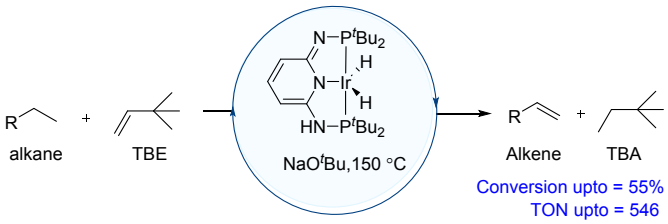

Figure 1. This Work: Alkane dehydrogenation catalysed by PN^{3}PIrH$_2$ complex.

To continue the study of these PN^{3}P-pincer iridium complexes, we synthesized **Ir1**, I**r2** and **Ir3** according to a previously reported method.[54] To test the performance of these catalysts for dehydrogenation reaction, we started the dehydrogenation reaction of cyclooctane (COA) as a model substrate and *tert*-butylethylene (TBE) as the sacrificial hydrogen acceptor. We conducted the reaction of cyclooctane (3.0 mmol), TBE (3.0 mmol) with sodium *tert*-butoxide (NaO^{t}Bu) as a base and **Ir1** catalyst (3.0 µmol, 0.1 mol%). The reaction mixture was heated at 150 °C in a closed reaction tube. The reaction was monitored by GC-MS as well as ^{1}H-NMR, and we observed after 24h, the formation of cyclooctene (COE) as well as trace amount of 1,3-cyclooctadiene (1,3-COD) product with overall conversion of 10% and TON was achieved up to 99 (Table

Entry	[Ir]:COA	[Ir]:TBE	Temp.	Conv. (%)^b	TON^b
1	1000	100	150	5	3
2	1000	500	150	24	118
3	1000	1000	150	55	546

1, entry 1). Next, we studied the performance of dearomatized PN^{3}P pincer dihydride iridium complex, **Ir2**. Surprisingly, in the case of **Ir2** catalyst under similar reaction conditions, gave 55% conversion with TON up to 546 (Table 1, entry 2). When **Ir3** catalyst was tested under similar reaction conditions, it shows conversion of 40% with TON up to 403 (Table 1, entry 3). Next, we studied the effect of oxidants to tune the oxidation potentials, for example ferrocenium salts, [Fe]$^+$[BF$_4$]$^-$ for alkane dehydrogenation reactions.[24] We observed that the addition of [Fe]$^+$[BF$_4$]$^-$ salt (Fe= Ferrocenium) to the reaction mixture enhanced the conversion for all Ir catalyst by 2-6% respectively. (Table 1, entries 4-6). Next, we examined the effect of another base such as potassium *tert*-butoxide (KO^{t}Bu) with and without adding of [Fe]$^+$[BF$_4$]$^-$ which gives a slightly lower conversion as compared to NaO^{t}Bu (Table 1, entries 7-8).

Table 1 Optimization reaction conditions towards cyclooctane dehydrogenation.[a]

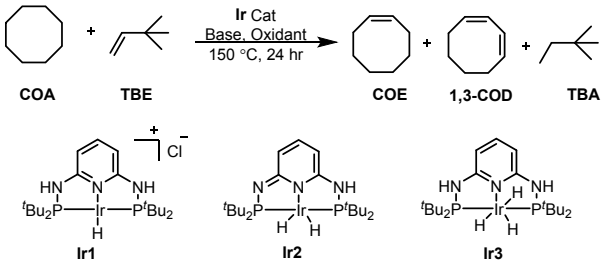

Entry	Ir cat.	Base	Oxidant	Conv. (%)^b	TON^b
1	**Ir1**	NaO^{t}Bu	-	10	99
2	**Ir2**	NaO^{t}Bu	-	55	546
3	**Ir3**	NaO^{t}Bu	-	40	403
4	**Ir1**	NaO^{t}Bu	[Fe]$^+$[BF$_4$]$^-$	16	157
5	**Ir2**	NaO^{t}Bu	[Fe]$^+$[BF$_4$]$^-$	56	558
6	**Ir3**	NaO^{t}Bu	[Fe]$^+$[BF$_4$]$^-$	42	415
7	**Ir2**	KO^{t}Bu	-	48	481
8	**Ir2**	KO^{t}Bu	[Fe]$^+$[BF$_4$]$^-$	50	502

[a]For the reaction, alkane (3.0 mmol),TBE (3.0 mmol), **Ir cat** (3.0 µmol, 0.1 mol%), base (15.0 µmol, 0.5 mol%), oxidant (15.0 µmol, 0.5 mol%) were heated in an autoclave. [b]Determined by GC using mesitylene as an internal standard. TON were calculated based on conversion of TBE determined by GC.

The concentration of TBE also plays a crucial role in driving the reaction of dehydrogenation of COA forward. We studied different ratio of **Ir2:**TBE:COA as shown in the Table 2. When the reaction is carried out with the ratio of 1:100:1000 of **Ir2:**TBE:COA, it resulted in 5% conversion with TON up to 3 (Table 2, entry 1). The conversion of dehydrogenation of COA was increased to 24% when the ratio of TBE was increased to 1:500:1000 giving the TON up to 118 (Table 2, entry 2). A further increase of the ratio to 1:1000:1000, the conversion enhanced to 55% with higher TON up to 546 (Table 2, entry 3). This observation highlighted the importance of maintaining a sufficiently high molar ratio of TBE to COA to effectively scavenge hydrogen and shift the reaction equilibrium towards dehydrogenation.

Table 2 Optimization of the reaction conditions towards cyclooctane dehydrogenation.[a]

[a]For the reaction, alkane (3.0 mmol), TBE (0.3-3.0 mmol) **Ir1 cat** (0.1 mol%), NaO^{t}Bu (15.0 µmol, 0.5 mol%) were heated in an autoclave. [b]Determined by GC using mesitylene as an internal standard. TON were calculated based on conversion of TBE determined by GC.

Further, we explored the dehydrogenation process with KO^{t}Bu and NaO^{t}Bu as base at different time intervals. In the case of KO^{t}Bu, the reaction was carried out initially for 4 h, and GC analysis of the reaction mixture showed a TBE conversion of 45% with a TON of up to 447 (Table 3, entry 1). Extending the reaction time to 16 h and 24 h further increased the TBE conversion to 47% and 48%, respectively, with corresponding TON up to 466 and 481 (Table 3, entries 2 and 3). While in the case of NaO^{t}Bu as base, for 4h, 16 h and 24h time intervals gave 49%, 50% and 55% of TBE conversion with TON up to 499, 501 and 546 respectively (Table 3, entries 4-6). This observation suggested that extending the reaction time for dehydrogenation reaction does not substantially improve catalytic activity of **Ir2**.

Table 3 Time dependent study for cyclooctane dehydrogenation.[a]

Entry	Time (h)	Base	Conv. of TBE (%)[b]	TON[b]
1	4	KO^{t}Bu	45	447
2	16	KO^{t}Bu	47	466
3	24	KO^{t}Bu	48	481
4	4	NaO^{t}Bu	49	499
5	16	NaO^{t}Bu	50	501
6	24	NaO^{t}Bu	55	546

[a]For the reaction, alkane (3.0 mmol), TBE (3.0 mmol), **Ir1 cat** (0.1 mol %), base (15.0 µmol, 0.5 mol%) were heated in an autoclave. [b]Determined by GC using mesitylene as an internal standard. TON were calculated based on conversion of TBE determined by GC.

Next, we studied the substrate scope using both linear and cyclic alkanes. The dehydrogenation of linear alkanes is particularly challenging because of the higher energy required for C–H activation compared to cyclic alkanes.[55] We initially explored n-octane as substrate. When the reaction was carried out using n-octane, **Ir2**, and NaO^{t}Bu in presence of TBE at 150 °C. After 15 h reaction time, the reaction was analyzed by GC which gives 15% TBE conversion. Along with 1-octene as the dehydrogenated product, we also observed trace amount of isomerized 2-octene and 1,2-dimethylcyclohexane (Table 4, entry 1). These results suggested that the linear alkane shows lower reactivity towards dehydrogenation reaction. Whereas the cyclic alkanes such as cyclohexane is effectively converted to cyclohexene with a yield of 10% (Table 4, entry 2). However, complete dehydrogenation product to form benzene was not observed. Next, we evaluated the 1,2,3,4-tetrahydronaphthalene as a bicyclic substrate. After the reaction, we observed the fully dehydrogenated naphthalene as a product with 25% total conversion along with 5% of partially dehydrogenated product, 1,4-dihydronapthalene (Table 4, entry 3).

Table 4 Substrate scope study.[a]

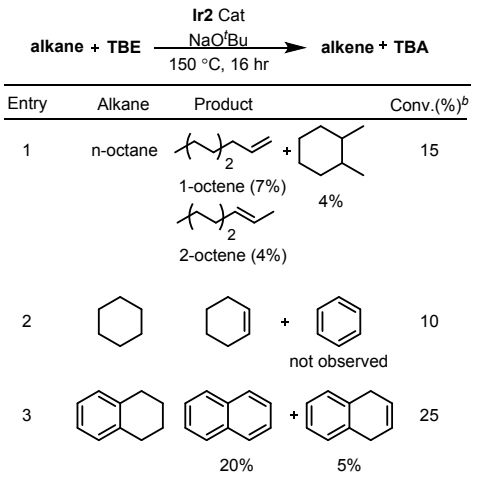

[a]For the reaction, alkane (3.0 mmol), TBE (3.0 mmol), **Ir1 cat** (0.1 mol %), NaO^{t}Bu (15.0 µmol, 0.5 mol%) were heated in an autoclave. [b]Determined by GC using mesitylene as an internal standard.

To shed light on the reaction mechanism, density functional theory (DFT) calculations by using Gaussian 16 suite[56] was performed (for more details, see the Supporting Information). As shown in Figure 2, the reaction cycle begins with the formation of catalytically active species **IN1**, resulting from the reaction of **Ir2** with the base NaO^{t}Bu along with loss of ^{t}BuOH. The active species **IN1** then forms a loosely bound adduct with TBE to form **IN2**, which is uphill by 5.7 kcal/mol. Next, the first hydrogen abstraction occurs at **IN2** to give **IN3** *via* three membered transition state **TS1**, with a free energy barrier of 29.7 kcal/mol. Subsequently, **IN3** undergoes the second hydrogen abstraction to generate Ir-catalyst (**IN4**) in its least oxidation state along with alkane having a transition state (**TS2**) barrier of 6.5 kcal/mol. Then, the complex **IN4** binds with the cyclooctane *via* σ-complex **IN5**, which is slightly exergonic by 3.9 kcal/mol. Next, **IN5** undergoes 1,2-addition of the C–H bond across the Ir catalyst to give cyclooctane intermediate **IN6**, traversing transition state **TS3** with a barrier of 10.2 kcal/mol. Finally, the β-hydride abstraction from the cyclooctyl group in **IN7** leads to formation of product cyclooctene (**COE**) along with regeneration of active catalyst **IN1**. These four membered transition states (TS4) required the transition state barrier of 11.8 kcal/mol. Overall, these calculations indicate that the alkene insertion is the rate determining step of the reaction with highest transition energy barrier of 29.7 kcal/mol.

View Article Online
DOI: 10.1039/D5NJ01050A

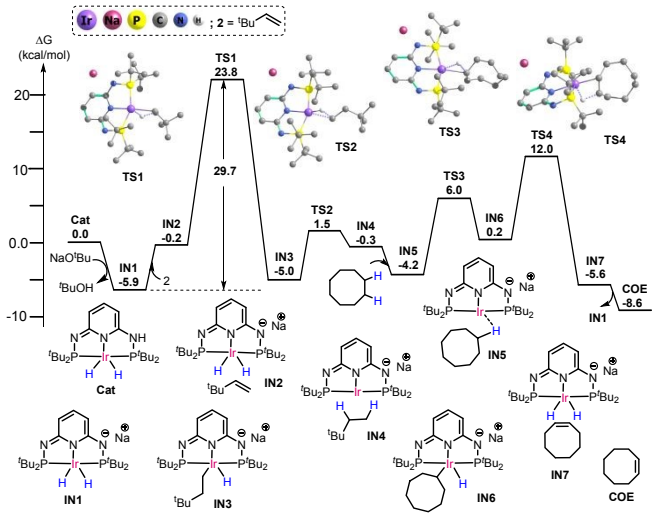

Figure 2. Free energy profile of dehydrogenation of cyclooctane using **Ir2** catalyst. Free energy values are at the M06/SDD(Ir)/def2-TZVP(C,H,O,N,P,Na)//BP86/SDD(Ir)/def2-SVP(C,H,O,N,P,Na) level of theory. Non-essential hydrogen atoms have been omitted for the sake of clarity.

After detailed DFT study, the possible reaction mechanism is illustrated as shown in Figure 3.[57] First step is the 16-electron iridium dihydride (**Ir2**) complex, insertion of TBE converts the alkyl hydride complex B which undergoes reductive elimination to form 14-electron C species. This complex activates the C–H bond of cyclooctane to give D species, followed by *β*-hydride elimination to yield cyclooctene and regenerate the **Ir2**.

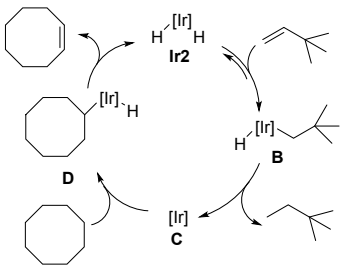

Figure 3. Possible reaction mechanism of COA with TBE using **Ir2**

Conclusion

PN^{3}P iridium complexes **Ir1**, **Ir2** and **Ir3** with 2,6-diamino phosphine ligands have been studied towards dehydrogenation of alkanes. The catalytic performance of PN^{3}P pincer iridium dihydride complex (**Ir2**) shows good performance in the dehydrogenation reaction of cyclooctane to cyclooctene. We achieved conversion up to 55% of *tert*-butylethylene (TBE) with TON up to 546. These results highlight the potential of PN^{3}P pincer iridium dihydride complex as a robust catalyst for selective alkane dehydrogenation under mild reaction conditions. DFT calculation shows that once the active species **I** formed after the treatment of NaO^{t}Bu which forms loosely bound adduct with TBE to form intermediate **II**, which is uphill by 5.7 kcal/mol. Given that TBE which is mono substituted olefin and highly selective for hydrogenation. Also, the dehydrogenation is turnover-limiting and alkene (TBE and COE) complexes are the resting states. When concentration of TBE is low, the hydrogenation is turnover-limiting and the resting state is **Ir1**, while at high [TBE], COA dehydrogenation is turnover-limiting, and the resting state is the vinyl hydride.

Acknowledgement

This work was supported by the Agency for Science, Technology and Research's (A*STAR) Council Strategic Fund C230415018 and the HTCO Seed Fund (C231218002). M.V.M. thanks the financial support by the ANRF (ANRF/ECRG/2024/002337/CS) and CNMS, Jain University, Bangalore, India.

Conflicts of interest

The authors declare no competing financial interest.

1. J. A. Labinger, D. C. Leitch, J. E. Bercaw, M. A. Deimund M. E. Davis, *Top Catal.* 2015, **58**, 494-501.
2. K. I. Goldberg, A. S. Goldman, *Acc. Chem. Res.* 2017, **50**, 620-626.
3. a) S. J. F. Sadrameli, *Acc. Chem. Res.* 2015, **140**, 102-115. b) T. Ren, M. Patel, K. Blok, *Energy* 2006, **31**, 425-451.c) M. Tuomaala, M. Hurme, A.M. Leino, *Appl. Therm. Eng.* 2010, **30**, 45-52.
4. K. Mazloomi, C. Gomes, *Renew. Sustain. Energy Rev.* 2012, **16**, 3024-3033.
5. a) G. Chen, T. Zhang, cMat, 2025. **2,** e12287 b) S. R. Patlolla, K. Katsu, A. Sharafian, K. Wei, O. E. Herrera, W. Mérida, *Renew. Sustain. Energy Rev.* 2023, **181**, 113323. c) A.C. Chang, H.F. Chang, F.J. Lin, K.H. Lin, C.H. Chen, *Int. J. Hydrog. Energy* 2011, **36**, 14252-14260.
6. H. Afeefy, NIST Chemistry Webook 2005.
7. a) A. Kumar, T. M. Bhatti, A. S. Goldman, *Chem. Soc. Rev.* 2017, **117**, 12357-12384. b) J. J. Sattler, J. Ruiz-Martinez, E. Santillan-Jimenez, B. M. Weckhuysen, *Chem. Rev.* 2014, **114**, 10613-10653. c) Z. Nawaz, *Rev. Chem. Eng.* 2015, **31**, 413-436.
8. a) M. J. Burk, R. H. Crabtree, *J. Am. Chem. Soc.* 1987, **109**, 8025-8032 b) D. Shee, A. Sayari, *Appl. Catal. A: Gen.* 2010, **389**, 155-164.
9. B. M. Gordon, N. Lease, T. J. Emge, F. Hasanayn, A. S. Goldman, *J. Am. Chem. Soc.* 2022, **144**, 4133-4146.
10. a) X. Jia, Z. Huang, *Nature Chem*. 2016, **8**, 157-161. b) F. Yu, R. Tao, Y. Su, G. Liu, Z. Huang, *Org. Lett.* 2022, **24**, 4563-4568.
11. R. H. Crabtree, M. F. Mellea, J. M. Mihelcic, J. M. Quirk, *J. Am. Chem. Soc.* 1982, **104**, 107-113.
12. M. J. Burk, R. H. Crabtree, C. P. Parnell, R. J. Uriarte, *Organometallics* 1984, **3**, 816-817.
13. M. Findlater, J. Choi, A. S. Goldman, M. Brookhart, In *Catal. Met. Complexes*, Springer, 2012, 113-141.
14. J. Choi, A. H. R. MacArthur, M. Brookhart, A. S. Goldman, *Chem. Rev.* 2011, **111**, 1761-1779.
15. M. C. Haibach, S. Kundu, M. Brookhart, A. S. Goldman, *Acc. Chem. Res.* 2012, **45**, 947-958.
16. a) M. Gupta, C. Hagen, R. J. Flesher, W. C. Kaska, C. M. Jensen, *Chem. Commun.* 1996, **17**, 2083-2084. b) M. Gupta, C. Hagen, R. J. Flesher, W. C. Kaska, C. M. Jensen, *Chem. Commun.* 1996, **17**, 2083-2084. c) J. Belli, C. M. Jensen, *Organometallics* 1996, **15**, 1532-

1534. d) M. Gupta, C. Hagen, W. C. Kaska, R. E. Cramer, C. M. Jensen, *J. Am. Chem. Soc.* 1997, **119,** 840-841. e) D. W. Lee, W. C. Kaska, C. M. Jensen, *Organometallics* 1998, **17**, 1-3. f) C. M. Jensen, *Chem. Commun.* 1999, **24** , 2443-2449. g) D. Morales-Morales, D. W. Lee, Z. Wang, C. M. Jensen, *Organometallics* 2001, **20,** 1144-1147. h) D. Morales-Morales, R. Redón, C. Yung, C. M. Jensen, *Inorg. Chim. Acta.* 2004, **357**, 2953-2956.

17. a) K. B. Renkema, Y. V. Kissin, A. S. Goldman, *J. Am. Chem. Soc.* 2003, **125**, 7770-7771. b) K. E. Allen, D. M. Heinekey, A. S. Goldman, K. I. Goldberg, *Organometallics* 2013, **32**, 1579-1582.
18. a) X. Zhou, S. Malakar, T. Dugan, K. Wang, A. Sattler, D. O. Marler, T. J. Emge, K. Krogh-Jespersen, A. S. Goldman, *ACS Catal.* 2021, **11**, 14194-14209. b) A. Parihar, T.J. Emge, F. Hasanayn, A.S. Goldman, *J. Am. Chem. Soc.* 2025, **147,** 10279-10297.
19. S. Kundu, Y. Choliy, G. Zhuo, R. Ahuja, T. J. Emge, R. Warmuth, M. Brookhart, K. Krogh-Jespersen, A. S. Goldman, *Organometallics*, 2009, **28**, 5432-5444.
20. A. Kumar, T. Zhou, T. J. Emge, O. Mironov, R. J. Saxton, K. Krogh-Jespersen, A. S. Goldman, *ACS Catal.* 2015, **137**, 9894-9911.
21. R. Ahuja, B. Punji, M. Findlater, C. Supplee, W. Schinski, M. Brookhart, A. S. Goldman, *Nature Chem.* 2011, **3**, 167-171.
22. B. Punji, T. J. Emge, A. S. Goldman, *Organometallics* 2010, **29**, 2702-2709.
23. A. Paul, C. B. Musgrave, *Angew. Chem. Int. Ed.* 2007, **46**, 8153.
24. A. D. R. Shada, A. J. Miller, T. J. Emge, A. S Goldman, *ACS Catal.* 2021, **11**, 3009-3016.
25. T. M. Bhatti, A. Kumar, A. Parihar, H. K. Moncy, T. J. Emge, K. M. Waldie, F. Hasanayn, A. S. Goldman, *J. Am. Chem. Soc.* 2023, **145**, 18296-18306
26. D. Milstein, *Philos. Trans. R. Soc. A* 2015, **373**, 20140189.
27. M. Rauch, S. Kar, A. Kumar, L. Avram, L. J. Shimon, D. Milstein, *J. Am. Chem. Soc. 2020*, **142**, 14513-14521.
28. J. R. Khusnutdinova, D. Milstein, *Angew. Chem. Int. Ed.* 2015, **54**, 12236-12273.
29. T.-F. Ramspoth, J. Kootstra, S. R. Harutyunyan, *Chem. Soc. Rev.* 2024, **53**, 3216-3223.
30. N. E. Smith, W. H. Bernskoetter, N. Hazari, *J. Am. Chem. Soc.* 2019, **141**, 17350-17360.
31. M. R. Elsby, R. T. Baker, *Chem. Soc. Rev.* 2020, **49**, 8933-8987.
32. E. Ben-Ari, G. Leitus, L. J. Shimon, D. Milstein, *J. Am. Chem. Soc.* 2006, **128**, 15390-15391.
33. a) E. Fogler, J. A. Garg, P. Hu, G. Leitus, L. J. Shimon, D. Milstein, *Chem. Euro. J.* 2014, **20**, 15727-15731. b) Q.-Q. Zhou, Y.-Q. Zou, S. Kar, Y. Diskin-Posner, Y. Ben-David, D. Milstein, *ACS Catal*. 2021, **11**, 10239−10245.
34. C. Gunanathan, D. Milstein, *Acc. Chem. Res.* 2011, **44**, 588-602.
35. H. Li, B. Zheng, K.-W. Huang, *Coord. Chem. Rev.* 2015, **293**, 116-138.
36. T. Shimbayashi, K. I. Fujita, *Catalysts* 2020, **10**, 635.
37. T. Zell, D. Milstein, *Acc. Chem. Res.* 2015, **48**, 1979-1994.
38. T. P. Gonçalves, I. Dutta, K.-W. Huang, *Chem. Commun*, 2021, **57**, 3070-3082.
39. Y. Pan, C. L. Pan, Y. Zhang, H. Li, S. Min, X. Guo, B. Zheng, H. Chen, A. Anders, Z. Lai, *Chem. Asian J.* 2016, **11**, 1357-1360.
40. M. H. Huang, J. Hu, K.-W. Huang, *J. Chin. Chem. Soc.* 2018, **65**, 60-64.
41. H. Li, Y. Wang, Z. Lai K.-W. Huang, *ACS Catal.* 2017, **7**, 4446-4450.
42. T. Chen, H. Li, S. Qu, B. Zheng, L. He, Z. Lai, Z.-X. Wang, K.-W. Huang, *Organometallics* 2014, **33**, 4152-4155.
43. S. S. Gholap, A. Al Dakhil, P. Chakraborty, H. Li, I. Dutta, P. K. Das, K.-W. Huang, *Chem. Commun.* 2021, **57,** 11815-11818.
44. S. B. Dawood, P. Chakraborty, L. Yang, K.-W. Huang, *Tetrahydron Lett.* 2025, **167**, 155664.
45. Y. Pan, C. L. Pan, Y. Zhang, H. Li, S. Min, X. Guo, B. Zheng, H. Chen, A. Anders, Z. Lai, *Chem. Asian J.* 2016, **11**, 1294-1294.
46. M. J. Ajitha, K.-W. Huang, *Organometallics* 2025, **44**, 2099-2106.
47. S. Qu, Y. Dang, C. Song, M. Wen, K.-W. Huang, Z.-X. Wang, *J. Am. Chem. Soc.* 2014, **136**, 4974-4991.
48. H. Li, T. P. Gonçalves, D. Lupp, K.-W. Huang, *ACS Catal.* 2019, **9**, 1619-1629.
49. T. P. Gonçalves, K.-W. Huang, *J. Am. Chem. Soc.* 2017, **139**, 13442-13449.
50. C. Guan, Y. Pan, E. P. L. Ang, J. Hu, C. Yao, M.-H. Huang, H. Li, Z. Lai, K.-W. Huang, *Green Chem.* 2018, **20**, 4201-4205.
51. L.-P. He, T. Chen, D.-X. Xue, M. Eddaoudi, K.-W. Huang, *J. Organomet. Chem.* 2012, **700**, 202-206.
52. Y. Pan, C. Guan, H. Li, P. Chakraborty, C. Zhou, K.-W. Huang, *Dalton Trans.* 2019, **48**, 12812-12816.
53. L. Alrais, S. S. Gholap, I. Dutta, E. Abou-Hamad, B. W. J. Chen, J. Zhang, M. N. Hedhili, J.-M. Basset, K.-W. Huang, *Appl. Catal. B - Environ.* 2024, **342**, 123439.
54. Y. Pan, C. Guan, H. Li, P. Chakraborty, C. Zhou, K.-W. Huang, *Dalton Trans.* 2019, **48**, 12812-12816.
55. X. Tang, X. Jia, Z. Huang, *Chem. Sci.* 2018, **9**, 288-299.
56. M. Frisch, *et. al.* Gaussian, Inc., Gaussian 16, Revision C.02, Wallingford CT, 2019.
57. D. Bézier, C. Guan, K. Krogh-Jespersen, A. S. Goldman M. J. Brookhart, *Chem. Sci.* 2016, **7**, 2579-2586.

DOI: 10.1039/D6NJ01950A

Data Availability Statement

The authors confirmed that the data supporting the findings of this study are available with the article and its supplementary material. Raw data that support the findings of the study are available from the corresponding author, upon reasonable request.